Liquid Crystallinity of a Biological Polysaccharide: The Levan/Water Phase Diagram

Anne E. Huber, Patrick S. Stayton, and Christopher Viney*

Molecular Bioengineering Program, Center for Bioengineering, WD-12, University of Washington, Seattle, Washington 98195

David L. Kaplan

Biotechnology Division, U.S. Army Natick Research, Development and Engineering Center, Kansas Street, Natick, Massachusetts 01760

Received September 10, 1993; Revised Manuscript Received November 18, 1993®

ABSTRACT: Boundaries on the phase diagram for aqueous solutions of levan (a branched polymer of fructose) were located quantitatively by transmitted light measurements performed with a UV–visible spectrophotometer. Data were collected in the range 10–70 °C; the minimum concentrations required for separation of a liquid crystalline phase and the minimum concentration required for a fully liquid crystalline solution were identified within this range. The liquid crystalline nature of the anisotropic phase was confirmed by transmitted polarized light microscopy. The boundaries of the biphasic region (separated isotropic and anisotropic phases) are parallel, and they have a positive slope, suggesting that phase separation is dictated by hard rod interactions and that conformational disorder decreases the rod axial ratio with increasing temperature.

Introduction

Levan[1] is a naturally occurring branched homopolysaccharide of D-fructose (Figure 1). It is produced as an ingredient of barrier slimes and as a food reservoir by microorganisms. It also occurs in a variety of monocotyledonous plant tissues, where it may confer cold and drought resistance as well as function as a food reserve.

Within the levan backbone and individual side chains, the monomers are joined by $\beta(2\rightarrow6)$ linkages, while the side chains are joined to the backbone via $\beta(2\rightarrow1)$ linkages. The fraction of residues incorporated in side chains, as well as the molecular weight, depends on both the source organism and the growth conditions.[1-4] For bacterial levans, up to 30% of the residues may occur in side chains,[3] while the weight-average molecular weight[4] may exceed 10^7 Da. Both parameters have significantly lower values in the case of plant levans.[1,5]

In general, the properties of levans are similar to those of dextrans. Levans therefore are viewed as a possible substitute for dextrans in applications that require a combination of low viscosity, high water solubility, biocompatibility, and susceptibility to acid hydrolysis. As such, levans may be used in industrial gums (to emulsify, stabilize, or sweeten foods). They have also been evaluated as a blood plasma extender, and they have been suggested as an encapsulating agent for pharmaceuticals, a carrier for fragrances, and a material for producing edible food coatings.[1,6] The controlled biosynthesis of levan in continuous bacterial culture[4] offers the possibility of large-scale production of levan with high purity and controlled molecular characteristics.

There are a number of advantages to carrying out processing operations such as film forming on polymers in the liquid crystalline state and to subsequently retaining orientational molecular order in the solidified product.[7-11] The advantages (relevant to coatings and packaging material) of such processing may include (1) the reduced viscosity and therefore enhanced processability of the liquid crystalline state, (2) facilitated production of microstructures in which molecules are extended and globally aligned, leading to enhanced stiffness and strength in the direction of alignment, (3) reduced susceptibility of the solid product to retraction when heated, and (4) the ability to capitalize on guest–host interactions to orient constituents of blends that are not themselves liquid crystalline. Ranges of composition and temperature in which a system is processable from the liquid crystalline state can be conveniently represented on a phase diagram; this paper addresses the experimental determination of such a diagram for the levan–water system.

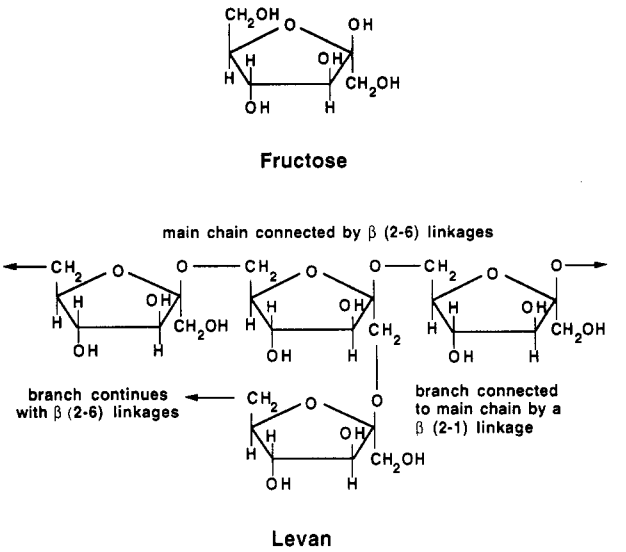

Figure 1. Schematic representation of levan and its fructose monomer.

The possibility that levan can form lyotropic liquid crystalline solutions is suggested by the turbidity of dilute solutions in water. This turbidity is apparent to the unaided eye and has been reported previously.[2] Also, computer modeling (of unbranched molecules) suggests that the molecular backbones have a helical and therefore rodlike structure.[12] We have used transmitted polarized light microscopy to confirm that a liquid crystalline phase is formed by aqueous levan solutions.[13] Liquid crystalline textures (a dense network of extinction bands, the positions of which change continuously as the crossed polars are rotated) were observed following partial drying of thin,

® Abstract published in *Advance ACS Abstracts*, January 15, 1994.

0024-9297/94/2227-0953$04.50/0

dilute samples maintained between a glass slide and cover slip. Neither the concentration at which anisotropic material first appears nor the concentration at which all isotropic material has disappeared can be measured accurately with this type of sample. Another limitation of polarized light microscopy is that liquid crystalline domains are not detected unless they coarsen to a scale greater than the instrumental resolution limit. Thus, it is possible for fine-textured biphasic or liquid crystalline samples to appear isotropic; they are more accurately characterized by small-angle light scattering.[14]

To accurately determine a phase diagram for levan in water, it is necessary to characterize the behavior of samples that (1) have a well-defined concentration and (2) are known to be homogeneous. Concentration can be maintained more accurately by working with larger sample volumes. Homogeneity is promoted if samples can be stirred, and can be monitored continuously if sample containers are transparent. We have accommodated these needs by using a UV–visible spectrophotometer to quantify turbidity as a function of temperature in samples of known concentration. A previous study (performed on aqueous solutions of (hydroxypropyl)cellulose) has demonstrated the viability of this approach,[15] although a quantitative phase diagram was not reported. The technique relies on the scattering of light at defects in the director field, where molecular orientation changes significantly over distances comparable to the wavelength of light. Relevant defects include disclinations and domain boundaries in liquid crystalline samples and also interfaces in biphasic samples. Therefore, if a single-phase isotropic solution is cooled until it is fully liquid crystalline, the most rapid increase in turbidity per unit temperature decrease occurs while the specimen is cooling through its biphasic range.

Materials and Methods

Levan, purified from a bacterial culture of *Erwinia herbicola*,[4] was obtained from the U.S. Army Natick Research, Development and Engineering Center (Natick, MA). The purified material was filtered to exclude molecular weights below 30 000 Da, and low-angle laser light scattering subsequently indicated a weight-average molecular weight of 2.97×10^7 Da.[4] Gel permeation chromatography (GPC) of levan prepared in this way provides estimates of polydispersity in the range 4–10; more accurate measurement is precluded by the inability of commercially available GPC columns to resolve the high molecular weight levan fractions.[16] Levan was dissolved in a 0.1 wt % aqueous sodium azide solution at the following concentrations (wt/wt): 1.0, 2.5, 3.0, 3.5, 4.0, 4.5, 5.0, 5.5, 6.0, 6.5, 7.5, and 10.0%. The sodium azide was added to eliminate bacterial growth in the vials. These concentrations were chosen after preliminary experiments had identified the concentration range in which significant phase transitions occur. Samples with concentrations above 10% levan were not tested, because their high viscosity precludes the preparation of homogeneous solutions.

A Hewlett-Packard 8452A UV–visible spectrophotometer was used to determine the relative turbidity of each solution as a function of temperature. The spectrophotometer was equipped with a thermostatable cell holder and magnetic cell stirring module attachment. A Neslab circulating water bath was used to control sample temperature and to drive the magnetic stirrer. An external thermometer (Fluke 51 K/J) and K-type thermocouple probe were used to measure temperature directly at the sample.

Aliquots (3–3.5 mL) of solution were pipetted into a quartz cuvette, and a stir bar was added. The cuvette was placed in the spectrophotometer cell holder and was covered with a lid to prevent evaporation. Samples were heated to 70 °C to aid initial mixing. An absorbance spectrum (averaged over 25 s) was collected for each sample at ca. 5 deg intervals as the temperature was decreased from 70 to 10 °C. Specimens were equilibrated for 10–15 min between measurements to ensure that the set point was reached. The cooling mechanism on the water bath allowed readings down to 15 °C; ice was added to the water for readings lower than this.

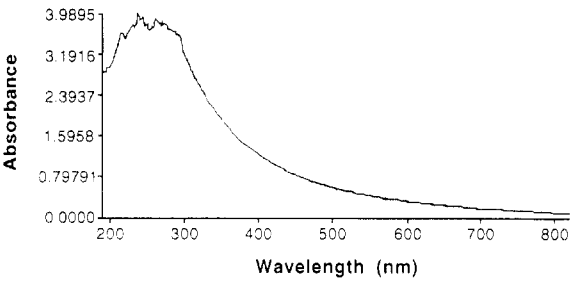

Figure 2. Typical absorption spectrum (raw data) acquired from the UV–visible spectrophotometer. The specimen was a 1 wt % solution of levan in water at 60 °C.

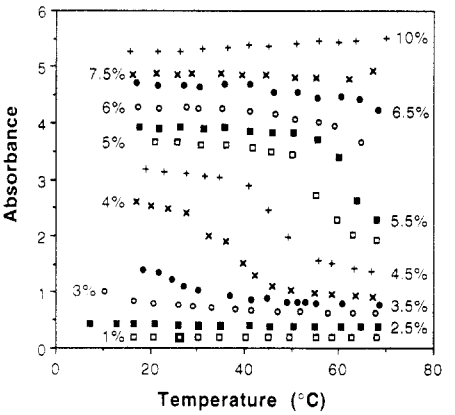

Figure 3. Absorbance at 700 nm for aqueous levan solutions (1–10 wt %) in the temperature range 10–70 °C. Data have been displaced along the absorbance axis to facilitate the representation of several data sets on a single diagram.

On selected samples, measurements were taken on the upward and downward ramping of the temperature to ensure that no hysteresis existed. In addition, measurements were repeated to verify reproducibility.

The liquid crystalline nature of selected samples was confirmed by transmited polarized light microscopy (Leitz Laborlux 12 POL).

Results and Discussion

The spectrophotometer output displays absorbance *versus* wavelength (between 190 and 820 nm); a typical example is shown in Figure 2. Absorbance is calculated as $\log(I_0/I)$, where I_0 is the light intensity incident on the sample and I is the intensity transmitted by the sample. Comparison of absorbance values for the purpose of phase diagram construction was made at 700 nm. In Figure 3, absorbance at this wavelength is plotted as a function of temperature for the various sample concentrations. These plots reveal three concentration ranges in which samples exhibit distinctly different phase transition behavior:

(1) At low concentrations (1 and 2.5% levan) the plots are relatively flat, suggesting that no phase transitions occur between 70 and 10 °C. Specimens viewed between crossed polars in a light microscope are isotropic. Bulk solutions appear slightly turbid to the unaided eye, as expected for solutions of a high molecular weight polymer.

(2) At intermediate concentrations (3.0–6.5% levan), the plots are sigmoidal. The solutions exhibit relatively little absorbance at high temperatures, consistent with isotropic molecular order. As a sample is cooled, a critical temperature is reached, below which the slope of the plot changes markedly. As the temperature continues to fall, there is a continuous, significant increase in absorbance, consistent with an increasing volume fraction of liquid

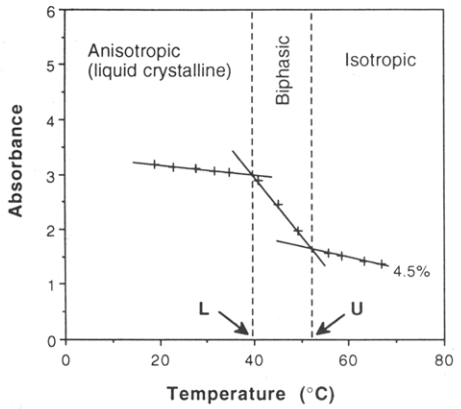

Figure 4. Illustration of how an absorbance *versus* temperature plot provides data for constructing a phase diagram. The readings for the 4.5 wt % solution are as shown in Figure 3. L and U are the lower and upper limits of the temperature range in which the sample turbidity changes most rapidly (due to a changing volume fraction of liquid crystalline material in the sample). These limits define the correspondingly labeled points in Figure 5.

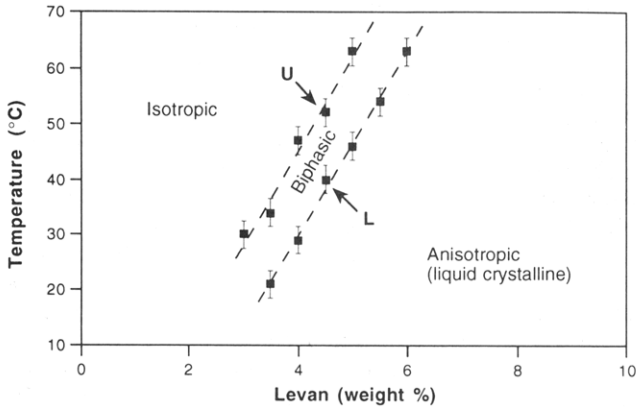

Figure 5. Levan–water phase diagram determined from the data in Figure 3, using the construction shown in Figure 4. Error bars represent the uncertainty in locating transition temperatures; the principal contribution to this uncertainty arises from the ca. 5 °C resolution of the data.

crystalline phase in the solutions. A second critical temperature is eventually reached, below which the plot levels off at a constant absorbance, suggesting that the entire volume of sample has become liquid crystalline. The critical temperatures at which the sigmoidal curves undergo the greatest change in slope (Figure 4) were used to develop the levan/water phase diagram (Figure 5).

(3) At still higher concentrations (7.5 and 10% levan) the plots again are relatively flat over the whole temperature range tested. The finite, approximately constant absorbance as a function of temperature, together with the turbid appearance of samples observed with the unaided eye, suggests that these solutions are liquid crystalline. Transmitted polarized light microscopy of thin specimens confined between a glass microscope slide and cover slip confirms the existence of liquid crystalline order (Figure 6). The fine scale of the microstructure, approaching optical resolution limits, is typical of schlieren textures in polymers.[11] The diffuse appearance of the texture is typical of viscous polymer liquid crystalline solutions and gels[17-21] (for example, solutions of many liquid crystalline cellulosics). A schlieren texture indicates either simple nematic molecular order or chiral nematic (cholesteric) molecular order with a large pitch.[22] The levorotatory nature of levan[1] and the computationally determined predisposition of levan to favor left-handed

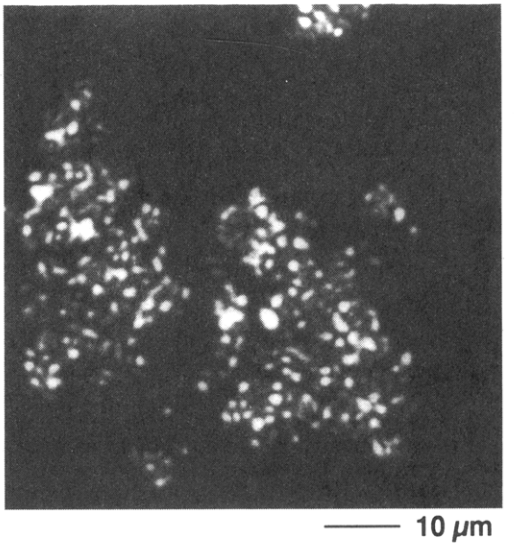

Figure 6. Liquid crystalline microstructure in droplets of a nominally 5 wt % solution of levan in water at ambient temperature. The specimen was maintained between a glass microscope slide and cover slip and was photographed between crossed polars. Initially, a definitive microstructure was not obtained; the texture was allowed to coarsen over a period of 2 days before it was photographed. The specimen appeared featureless when the polars were withdrawn from the microscope, confirming that contrast is due to optical anisotropy.

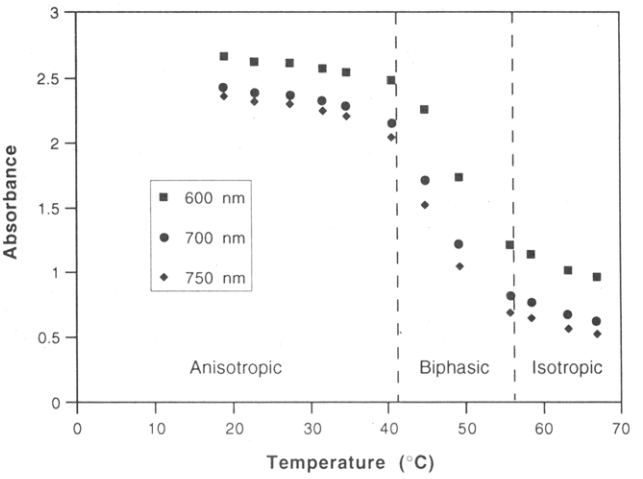

Figure 7. Absorbance at 600, 700, and 750 nm for a 4.5 wt % solution of levan in water.

helical conformations[12] suggest that the liquid crystalline phase is a chiral nematic.

The success of this method of phase diagram determination does not depend on specifically working with absorbance values measured at 700 nm. However, the choice of this wavelength takes account of various practical considerations. First, it is necessary to use data from the high-wavelength tail of the absorbance spectra to ensure a sensitive instrumental response (the response became saturated at or near the peak absorption). Second, by working at a wavelength far from the peak absorption, we can be confident that electronic transitions in either the levan or residual impurities do not contribute significantly to the measured absorbance. Third, the accuracy of the spectrometer photodiode array becomes questionable at the highest recorded wavelengths. A comparison of absorbance at 600, 700, and 750 nm plotted *versus* temperature for a sample of 4.5% concentration is shown in Figure 7. The variation in the phase boundaries as determined from data at these different wavelengths falls within the 5 °C error bars on the final phase diagram. We

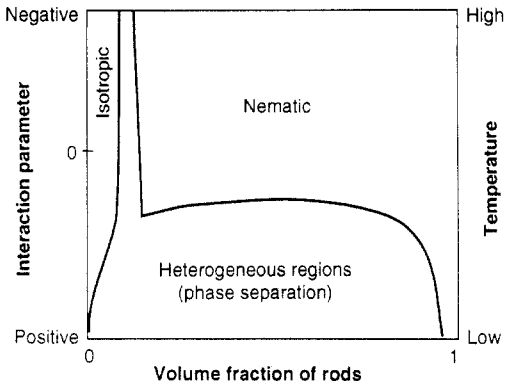

Figure 8. Phase diagram showing the existence of a single liquid crystalline phase, a single isotropic phase, or a heterogeneous mixture of phase-separated material predicted as a function of temperature (or interaction parameter) and concentration for rods with an axial ratio of 100. (Behavior of a non-athermal system; prediction used a simple lattice model.[23])

also note that previous investigators[15] used turbidity measurements at 700 nm when attempting to construct a phase diagram for (hydroxypropyl)cellulose–water, although no reasons are given for the choice of wavelength in this case.

Our experimentally determined phase diagram (Figure 5) corresponds to the "chimney" region of the well-known phase diagram predicted by Flory[23] for simple rod–solvent systems (Figure 8). The fact that the "chimney" in Figure 5 slopes to higher concentrations at higher temperatures implies that the axial (length-to-width) ratio of the rodlike component is a decreasing function of temperature. It is instructive to use the experimental diagram to estimate the rod axial ratio at various temperatures, as this value can be compared with the axial ratio of an entire molecule in the calculated[12] helical conformation. Thus, one can determine whether the rods are entire single molecules or statistically rigid (Kuhn) segments of single molecules. The rod axial ratio, x, at a given temperature can be estimated from the predicted relationship[23] between x and the critical rod volume fraction for incipience of *metastable* order in a solution, v^*:

$$v^* \sim \frac{8}{x}\left(1 - \frac{2}{x}\right) \tag{1}$$

This equation is accurate to within 2% for $x > 10$. Improvements in the sophistication of the lattice model from which this equation was derived led to the recognition[24,25] that eq 1 gives an even more accurate estimate of the minimum rod volume fraction required for *stable* order to arise in a solution. Equation 1 has been used to characterize the axial ratio of several semiflexible polysaccharides in lyotropic solution.[25,26] From Figure 5, v^* at 30 °C is ca. 3 wt %. The corresponding concentration in volume percent will be somewhat lower (because levan is more dense than water); in the absence of a value for the density of levan, we continue this order-of-magnitude calculation by simply interchanging weight percent and volume percent. Equation 1 can be rearranged to give

$$x \sim \frac{4}{v^*}[1 \pm (1 - v^*)^{1/2}] \tag{2}$$

Only the positive root is physically relevant. Substituting $v^* \sim 0.03$ gives $x \sim 265$. At 65 °C, $v^* \sim 0.05$ (Figure 5), for which eq 2 estimates $x \sim 158$. Published models of the possible range of helical conformations for levan[12] would require rodlike segments to have a mass between 2.1×10^5 and 6.7×10^5 Da if their axial ratio is ~265. For rods with an axial ratio of ~158, the mass would range between 1.2×10^5 and 4.0×10^5 Da. (It must be emphasized that the models[12] simply find *accessible* helix conformations; they do not take account of the potential for hydrogen bonding and therefore do not identify a single most likely or stable conformation. However, it is likely that significant intramolecular hydrogen bonding is needed to make a helical conformation persist to the large axial ratios reported above.) Since the weight-average molecular weight of our levan[4] is 2.97×10^7 Da, it is apparent that the rods which dominate phase separation are statistically rigid segments of individual molecules—even allowing for the underestimation of axial ratio that follows from interchanging weight percent and volume percent concentrations. With increasing temperature, conformational disorder increases, favoring rods with a smaller axial ratio and requiring a higher concentration to stabilize liquid crystalline order.

Conclusions

1. Absorbance measurements by UV–visible spectrophotometry enable quantitative location of boundaries on the levan–water phase diagram. At 20 °C, solutions are fully liquid crystalline above 3.5 wt % levan.

2. Between 30 and 65 °C, solutions are biphasic (separate into isotropic and anisotropic phases) over a narrow concentration range of approximately constant width; the biphasic range is displaced continuously toward higher concentrations as temperature increases. This behavior is characteristic of a lyotropic solution in which phase separation is dictated by hard rod interactions.

3. The estimated magnitude of the rod axial (length-to-width) ratio suggests that the rods which dominate phase separation are statistically rigid segments of molecules rather than entire molecules.

4. The axial ratio of the rods decreases with increasing temperature, indicative of increasing conformational disorder.

Acknowledgment. The authors are grateful to Alfred Allen for providing samples of levan and to Dr. Paul Yager for useful discussions and the loan of equipment. Support was provided by the U.S. Army Natick RD&E Center (Contract No. DAAK60-91-K-005) and the 3M Co.

References and Notes

(1) Han, Y. W. In *Advances in Applied Microbiology*, 1st ed.; Neidleman, S. L., Laskin, A. I., Eds.; Academic Press: San Diego, 1990; Vol. 35, p 171.
(2) French, A. D. *J. Plant Physiol.* **1989**, *134*, 125.
(3) Simms, P. J.; Boyko, W. J.; Edwards, J. R. *Carbohydr. Res.* **1990**, *208*, 193.
(4) Keith, J.; Wiley, B.; Ball, D.; Arcidiacono, S.; Zorfass, D.; Mayer, J.; Kaplan, D. *Biotechnol. Bioeng.* **1991**, *38*, 557.
(5) Tomasic, J.; Jennings, H. J.; Glaudemans, C. P. J. *Carbohydr. Res.* **1978**, *62*, 127.
(6) Kaplan, D. L.; Mayer, J. M.; Ball, D.; McCassie, J.; Allen, A. L.; Stenhouse, P. In *Biodegradable Polymers and Packaging*, 1st ed.; Ching, C., Kaplan, D. L., Thomas, E. L., Eds.; Technomic: Lancaster, PA, 1993; p 1.
(7) Cox, M. K. *Mol. Cryst. Liq. Cryst.* **1987**, *153*, 415.
(8) Ryan, T. G. *Mol. Cryst. Liq. Cryst.* **1988**, *157*, 577.
(9) Collings, P. J. *Liquid Crystals: Nature's Delicate Phase of Matter*; Princeton University Press: Princeton, NJ, 1990.
(10) Weiss, R. A.; Ober, C. K., Eds.; *Liquid-Crystalline Polymers*, 1st ed.; American Chemical Society: Washington, DC, 1990; Vol. 435.
(11) Donald, A. M.; Windle, A. H. *Liquid Crystalline Polymers*, 1st ed.; Cambridge University Press: Cambridge, 1992.
(12) French, A. D. *Carbohydr. Res.* **1988**, *176*, 17.
(13) Viney, C.; Huber, A.; Verdugo, P. In *Biodegradable Polymers and Packaging*, 1st ed.; Ching, C.; Kaplan, D. L., Thomas, E. L., Eds.; Technomic: Lancaster, PA, 1993; p 209.

(14) Rojstaczer, S.; Stein, R. S. *Mol. Cryst. Liq. Cryst.* **1988**, *157*, 293.
(15) Fortin, S.; Charlet, G. *Macromolecules* **1989**, *22*, 2286.
(16) Arcidiacono, S., private communication, 1993.
(17) Chanzy, H.; Peguy, A.; Chaunis, S.; Monzie, P. *J. Polym. Sci., Polym. Phys. Ed.* **1980**, *18*, 1137.
(18) Zugenmaier, P.; Vogt, U. *Makromol. Chem.* **1983**, *184*, 1749.
(19) Dayan, S.; Gilli, J. M.; Sixou, P. *J. Appl. Polym. Sci.* **1983**, *28*, 1527.
(20) Viney, C.; Windle, A. H. *Mol. Cryst. Liq. Cryst.* **1987**, *148*, 145.
(21) Rout, D. K.; Pulapura, S. K.; Gross, R. A. *Macromolecules* **1993**, *26*, 5999.
(22) Demus, D.; Richter, L. *Textures of Liquid Crystals*, 1st ed.; Verlag Chemie: Weinheim, 1978.
(23) Flory, P. J. *Proc. R. Soc. London* **1956**, *A234*, 73.
(24) Flory, P. J.; Ronca, G. *Mol. Cryst. Liq. Cryst.* **1979**, *54*, 289.
(25) Flory, P. J. *Adv. Polym. Sci.* **1984**, *59*, 1.
(26) Gray, D. G. *J. Appl. Polym. Sci., Appl. Polym. Symp.* **1983**, *37*, 179.